buildings

MDPI

Article

Alternative Use of the Waste from Ground Olive Stones in Doping Mortar Bricks for Sustainable Façades

Alejandro San Vicente-Navarro [1], Manuel Mendívil-Giro [2], Jorge Los Santos-Ortega [1,*], Esteban Fraile-García [1] and Javier Ferreiro-Cabello [1]

[1] SCoDIP Group, Department of Mechanical Engineering, University of La Rioja, 26004 Logroño, Spain; alejandro.san-vicente@unirioja.es (A.S.V.-N.); esteban.fraile@unirioja.es (E.F.-G.); javier.ferreiro@unirioja.es (J.F.-C.)

[2] GI-TENECO Group, Department of Mechanical Engineering, University of La Rioja, 26004 Logroño, Spain; manuel-antonio.mendivil@unirioja.es

* Correspondence: jorge.los-santos@unirioja.es

Abstract: The aim of achieving sustainability in construction is a reality. A useful strategy to achieve this is the use of waste from agricultural activities. This waste could reduce the environmental impacts associated with the production of raw materials such as natural aggregate, reducing energy consumption from fossil fuels and therefore CO_2 emissions. This study examines the thermal conductivity of mortars doped with ground olive stones, a residual by-product of industrial processes. The objective is to evaluate the potential of ground olive stones to improve thermal insulation in construction. Ground olive stones are used as a partial replacement for the aggregates used in mortar bricks. The methodology followed herein to quantify the benefits of this product involves creating several types of mortar with a different percentage of ground olive stones in each sample (between 0% and 30%). Thermal conductivity was determined according to UNE-EN12939:2001. Finally, a case study is conducted performing an energy simulation of a residential building to determine the energy savings derived from reducing the combined thermal demands of heating and cooling and to analyse the feasibility of the alternative use of ground olive stone residue doped in mortar bricks for new sustainable façades. The results show a saving in energy demand (heating and cooling) of 0.938 kWh/m^2·year when using 30% GOS-doped mortar bricks compared to the reference bricks. This is equivalent to a decrease in energy demand of 2.23% per square meter of façade. In addition, these annual energy savings are compared to the potential thermal energy created from the combustion of ground olive stones in a biomass boiler, which is the main traditional use of this waste today. It reveals that for a doping range of 5–15%, the recovery time ranges between 30 and 75 yeas, which is within the lifetime of a building. The results demonstrate the great viability of using ground olive stones as fine aggregates in mortars and their possible application in sustainable construction, in particular in more sustainable façades that allow energy savings in buildings and therefore a lower consumption of fossil, which will make it possible to reduce greenhouse gas emissions and the excessive consumption of resources.

Keywords: thermal conductivity; ground olive stone; mortar; perforated brick; façade; sustainability

Citation: San Vicente-Navarro, A.; Mendívil-Giro, M.; Los Santos-Ortega, J.; Fraile-García, E.; Ferreiro-Cabello, J. Alternative Use of the Waste from Ground Olive Stones in Doping Mortar Bricks for Sustainable Façades. *Buildings* **2023**, *13*, 2992. https://doi.org/10.3390/buildings13122992

Academic Editor: Antonio Caggiano

Received: 16 October 2023
Revised: 7 November 2023
Accepted: 28 November 2023
Published: 30 November 2023

1. Introduction

Recycling waste and reducing fossil fuel consumption are pillars of the global strategy to combat the effects of climate change and global warming. Until recently, the majority of waste generated by human activities was deposited in landfills without further treatment or additional uses. Only within recent years have various industrial processes been launched to reincorporate and reuse waste and by-products with a clear mission to implement a so-called circular economy [1]. Minimizing waste and reducing the consumption of raw materials are some of the key objectives of this framework. The construction sector is an

ideal area to test out the idea of a circular economy, given that new mixed materials can be developed by incorporating waste from other processes (sometimes hailing from outside the sector). Adding such residues can improve some properties of the final product.

Concrete and mortar are two of the most important construction products, mainly due to their excellent mechanical properties, durability, mouldability, and availability. Their annual production is estimated at over ten thousand million tons [2]. However, the intensive use of mortar and concrete in the construction sector also entails a significant environmental impact. It is estimated that the cement industry (the main component in concrete) is responsible for around 7% of annual CO_2 emissions [3]. And globally, the construction sector accounts for 36% of global energy consumption [4]. Therefore, the natural trend for the sector in line with the new global climate change guidelines is to decarbonise the sector [5]. It is therefore essential to work on gradually substituting or evolving cement by incorporating other compounds or materials that reduce the aforementioned environmental impact while offering similar or better properties (strength, thermal, acoustic, etc.). Repurposing products traditionally considered waste in other industrial processes would promote a circular economy and represent an undeniable improvement.

Other studies have already corroborated the viability of replacing certain natural aggregates with concrete waste from demolition or by-products from the concrete industry itself [6–8] in order to apply it, for example, in lightweight concrete [9]. Mortar and concrete mixes capable of enhancing thermal insulation deserve special mention. Since the end of the 20th century, European guidelines on energy efficiency [10,11] have called for reducing energy consumption in buildings while maintaining low operating costs and without sacrificing comfort. This leads them to design building elements with higher thermal insulation performance. For instance, Parracha et al. evaluated the feasibility of doping mortars with insulating elements as a substitute for fine aggregates and their application in a prototype wall. The results show a decrease in the thermal conductivity of the material and, therefore, energy savings [12].

Thus, many recycled materials have already been used experimentally as additives to concrete with the goal of optimising thermal behaviour. Some examples include plastics from different sources and compositions [13–16]. For instance, research by Todaro et al. evaluated the potential of using Polyethylene Terephthalate (PET) from waste bottles without any treatment as a substitute for conventional aggregates in mortars. The results show that mortars with PET have a better response to energy absorption and tensile strength, as well as an increase in thermal insulation in the range of 65–84% better than the reference mortar [13]. In the field of plastics, rubber waste from end-of-life tyres is also found [17–20]. However, this waste is not only focused on improving the thermal behaviour of mortar or concrete but also on other properties. Such is the case of the research by Eskander et al., where they develop cement–polymer composites from polystyrene foam waste fractions with the aim of improving mechanical durability and the porosity of the cement [21]. Other types of waste include waste from the cement industry itself. The dust obtained in the cement production kiln itself is used as an additive in compressed earth blocks [22] or the sludge obtained from the water purification process is used to produce bricks without any amount of clay [23]. Several different studies have also been conducted with agricultural residues, such as: barley fibres [24–26], banana leaf ashes and fibres [27–29], peanut shells [30,31], cork particles [32–34], sawdust ashes [35–37], sugarcane bagasse ash [38–40], rice husk ash [41,42], and olive ash [33,43], and waste wood [44,45]. In the case of the use of wood waste, this is very similar to olive waste since, in comparison with natural aggregates, there is a significant difference in the densities. This is evidenced in the research of Ince et al., where they use wood waste powder as a substitute for mortar cement. The results show a loss in the mechanical properties of the doped mortars; however, this decrease is affordable for construction elements. On the other hand, the improvement in the environmental characteristics is highlighted, since a doping percentage of 5% means a reduction in CO_2 emissions of 10%, which confers an environmental advantage [44]. And the same applies to other bio-based elements [46]. As can be seen, the use of agricultural waste in the construction

sector is a technique that is becoming more and more widespread and applied. In the present study, the goal is to use ground olive stones (GOSs), a biomass residue, as a substitute for fine aggregates.

Olive stones are a by-product from the agri-food industry (olive oil industry) that are considered waste. This biomass residue is generated after all the oil has been extracted from the olive. Given that olive trees need to grow in relatively hot climates, in Europe, they are primarily found in Greece, Italy, and Spain (where summers are dry and hot, and winters are cold and slightly humid). The latter is the largest producer of olives in the world, with Spanish production constituting around 75% of the global total, at close to 6 million tons each year. Half of this production is dedicated to oil production, and thus, olive stones become a residue of this process. An olive stone is estimated to be 15% of the total weight of an olive; therefore, around 450,000 tons of olive stone are generated every year in Spain [47].

Olive stone residue is currently repurposed as biofuel in biomass boilers thanks to its high calorific value (approximately 4489 kWh/kg, according to the Institute for Energy Diversification and Saving, IDAE). It is also considered a renewable fuel with zero net CO_2 emissions throughout the life cycle of an olive tree. It is used as a heat source in homes, farms, food sector industries, and collective-use buildings (elderly homes, schools, administrative buildings, etc.). However, new uses are already being proposed for olive waste other than as biomass. Some of them are applied to the construction sector, and others to wastewater treatment. In the case of wastewater treatment, Abdelhamid et al. used a mixture of dried olive residues together with hyacinth to decontaminate wastewater containing cobalt and caesium in a stable and radioactive state [48].

However, previous studies proposed to use this residue in mortars and to study its thermal properties. The research evaluated by Barreca et al. studied the use of GOSs as a substitute for fine aggregates in conventional mortars in order to characterise their thermal transmittance. The authors proposed a dosage range of 0–70% GOSs in increments of 10% and 20% intervals. The results showed a reduction in thermal transmittance ($W/m^2 \cdot K$) of 76% compared to a conventional mortar for a maximum doping range of 70%. They also indicated that, although the thermal transmittance was reduced, other physical properties such as density were also reduced (31% decrease for a doping of 70% GOSs). A maximum limit is proposed for the use of GOSs in mortars, since higher doping leads to instability of the mixture. Furthermore, they point out that this residue applied to the construction sector would be suitable for lightening elements and plaster layers to insulate walls and bricks [43].

The present study evaluates using GOSs to manufacture mortar with the goal of improving its thermal behaviour as an insulator. The main objective is to evaluate the thermal conductivity ($W/m \cdot K$) of GOSs in mortars. However, in contrast to the study by Barraca et al., in this research, the doping range (0–30%) is considerably narrowed down, studying within this interval the possible variations that exist in small increments (5%) in order to obtain a series of data with the smallest possible deviation. In addition, considerations in terms of the mechanical strength (compression and bending) of the mortars were taken into account [49]. In order to find out whether these doped mortars have a minimum of structural safety for their application to prefabricated elements, the heat transfer capacity (thermal conductivity) is analysed in the various samples and tested in a laboratory using a machine designed to measure the thermal conductivity of different construction materials. This procedure verifies whether doping mortars with GOSs leads to an improvement in thermal insulation as compared to the original undoped mortar. Once the results of the thermal conductivity ($W/m \cdot K$) of the mortar as a function of the levels of use of GOSs are obtained, we proceed to evaluate its application in the construction sector and quantify its advantages. To do this, a simulation of a residential building is carried out in which the façade is made using bricks doped with GOSs. In this way, its performance can be compared with that of a façade made with conventional bricks. Therefore, based on the results obtained, it is possible to justify a new use for this waste

and not its traditional destination, which is its combustion to obtain thermal energy. A reduction in the energy demands (heating and cooling) of the building is demonstrated when the façade is constructed with GOS-doped mortar bricks. The novelty obtained from this research lies in its ability to give conventional waste obtained as a result of the execution of an agricultural activity a new use, especially in the construction sector. This waste is converted back into raw materials, generating a circular economy that will help to obtain a more sustainable sector for society and the environment without losing the minimum safety and comfort properties for users.

2. Materials and Methods

2.1. Materials

The following materials are necessary to manufacture different samples of mortar doped with GOSs.

2.1.1. Fine Aggregates

Fine aggregates were used to manufacture mortars of the type AF-T-0/4-C with a maximum size of 4 mm and a density of 1634 kg/m^3. Figure 1 shows the cumulative percentage of fine aggregate obtained through a sieve analysis according to EN 933-1 [50]. Their technical characteristics are shown in Table 1. In this study, the source of the fine aggregates is crushed limestone from a local quarry, stored upon receipt at ambient conditions (20 °C and 55% relative humidity).

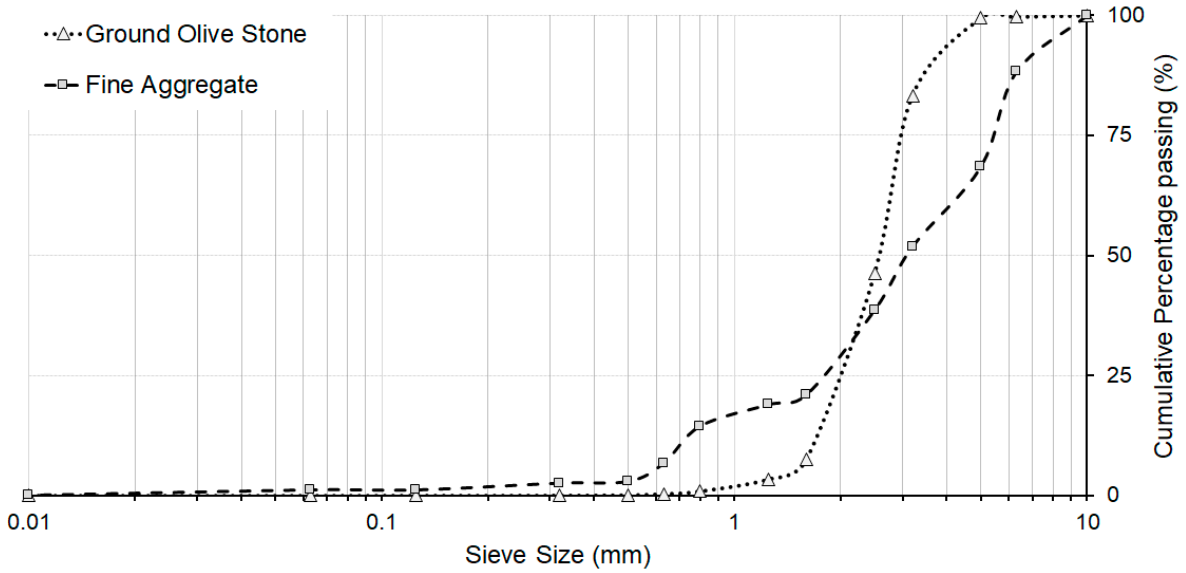

Figure 1. Fine aggregate and GOS granulometry.

Table 1. Technical characteristics of fine aggregates.

Tests	Results	Limits
Clay lumps, UNE 7-133 [51]	0.00%	<1%
Total sulphur compounds, UNE-EN 1744 [52]	0.082%	<1%
Water absorption by fine aggregate, UNE-EN 1097-6 [53]	1.19%	≤5%
Chlorides expressed in Cl^-, UNE-EN 1744 [52]	0.001%	≤0.05%
Acid soluble sulphates, UNE-EN 1744 [52]	0.052%	<0.08%

2.1.2. Water

Water is extracted from the supply network without any additional treatment; it has a pH of 7.9 and a sulphur content of 590 ppm.

2.1.3. Ground Olive Stone

Traditional mortars do not include this material, but in the case of this study, GOSs are used to dope and create different types of mortars. Thus, it is a key material in this study. The GOSs used herein were obtained from the company Trujal 5 Valles, located in Arnedo (La Rioja, Spain). This cooperative is the main olive producer in the region, and for this reason, its production surpasses demand. The ground olive stones have not undergone any type of chemical transformation; they are simply GOSs obtained after grinding olives in the olive oil extraction process. These GOSs are processed through a natural drying process, removing excessive moisture content. An example of the GOSs is shown in Figure 2.

Figure 2. GOSs used into dope mortar.

The chemical composition is shown in Table 2. The GOSs have a density of 580.07 kg/m^3. Their dimensions range between 1 and 4 mm, similar to those of the fine aggregates used. Figure 1 shows the cumulative percentage of GOSs found through a sieve analysis according to EN 933-1 [50].

Table 2. Chemical composition of GOSs.

Composition		Percentage
Chemical composition	C (%)	50.2
	O (%)	45.2
	H (%)	7.02
	N (%)	0.47
	S (%)	0.04
By component	Lignin (%)	32.1
	Hemicellulose (%)	34.8
	Cellulose (%)	26.9
	Soluble (%)	5.4
	Ash (%)	0.8

2.1.4. Cement

This product is obtained by mixing various elements, such as limestone and clay, to which a small amount of gypsum is added, along with other compounds. These are all ground together to obtain an extremely fine material.

The cement used herein is CEM II/B-M (V-L) 32.5 N from the brand Cements Portland Valderrivas (Madrid, Spain). It has a clinker percentage between 65% and 79%. This is a mix (between 21% and 35%) since it contains between 1% and 16% fly ash and between 0% and 20% limestone. It may also contain minor additional components, ranging from 0% to 5%. It has an initial strength of $\geq$16.5 MPa and a normal strength at 28 days between 32.5

and 52.5 MPa. The chemical composition of the material, supplied by Cements Portland Valderrivas S.A., is displayed in Table 3.

Table 3. General composition of Portland Valderrivas cement.

Material	Composition	Result (%)
Cementitious materials	SiO_2	18.05
	CaO	62.96
	MgO	2.07
	Al_2O_3	5.43
	Fe_2O_3	1.53
	SO_3	3.08
	Loss on ignition	5.04

2.2. Samples Preparation

Since in this research, the use of GOSs is as a substitute for the volume of the total fine aggregates, different replacement percentages were proposed. These percentages vary between 0% and 30% of the total fine aggregate volume. Given also the differences in water absorption and our objective being to obtain mortars with a constant consistency, class S2, according to UNE-EN-12350-2 [54], the amount of water is modified as the amount of GOS increase [49]. These amounts of water for each mortar sample can be seen in Table 4 and vary according to the doping percentage of the mortar. It is important to bear in mind that increasing the percentage of GOSs diminishes the compressive strength the different mortars are capable of withstanding. This fact is reported in the research carried out by Ferreiro et al., where they evaluate the mechanical and physical characteristics (density, compression, and flexural strength) of GOS-doped mortars with different CEM II cements. For the specific case of using CEM II 32.5R, they indicate a GOS use range of 0–30% [49]. For this reason, only a range of GOS use in mortars of 0–30% is studied in this research.

Table 4. Type and quantity of material used to manufacture of mortar mix.

Sample	Fine Aggregate (kg)	Cement (kg)	Water (kg)	GOSs (kg)
M-0	40.0	8.0	6.50	0.00
M-5	38.0	8.0	6.33	0.71
M-10	36.0	8.0	6.16	1.42
M-15	34.0	8.0	5.99	2.13
M-20	32.0	8.0	5.82	2.84
M-25	30.0	8.0	5.65	3.55
M-30	28.0	8.0	5.48	4.26

This issue restricts the use of olive stones in construction, and for this reason, the thermal samples are made with a maximum percentage of 30% GOSs. The mix names are identified as the volume percentage of fine aggregates substituted by GOSs. The following percentages are examined:

- M-0: 100% fine aggregate.
- M-5: 95% fine aggregate + 5% GOS.
- M-10: 90% fine aggregate + 10% GOS.
- M-15: 85% fine aggregate + 15% GOS.
- M-20: 80% fine aggregate + 20% GOS.
- M-25: 75% fine aggregate + 25% GOS.
- M-30: 70% fine aggregate + 30% GOS.

Samples of mortar measuring 0.30 m × 0.30 m × 0.05 m are created. Fine aggregates are used in the conventional manufacturing process of undoped mortar. The rest of the materials, water, cement, and GOSs, are used to dope the mortar.

Three different batches are manufactured (L1, L2, and L3), each consisting of two samples for all the different doping ratios. In all, six samples are made for each of the seven types of mortar. These types differ according to the percentage of GOSs they contain.

The amounts used of each material are listed in Table 4, depending on the percentage of ground olive stones used (0%, 5%, 10%, 15%, 20%, 25%, and 30%). The values in Table 4 correspond to the quantities of materials used for the creation of each mortar mix.

2.2.1. Mould Assembly

Before the assembly process, each of the moulds is cleaned, and a uniform layer of liquid release agent is applied to them with a brush to facilitate their extraction. Subsequently, the screws are inserted into the moulds.

2.2.2. Mould Filling

Once the moulds were prepared, they were filled with the mortar. Beforehand, the mortar underwent an Abrams cone test to determine if the mix was viable or not. Only mortars that passed this test were utilised. The moulds were filled in two pours to improve product vibration. The first vibration was conducted when each mould was half-full, and the second when the mould was completely full. And lastly, each mould was levelled off with a trowel.

2.2.3. Curing Process, Demoulding and Coding Samples

The minimum curing time was 24 h (1 day), although the samples ended up staying in the moulds for 3.5 days (approximately 84 h). The moulds were left uncovered (Figure 3) to dry inside an industrial warehouse protected from solar radiation and rain and completely sheltered from inclement weather. The temperature did not fluctuate very much from day to day (generally, the temperature inside the industrial warehouse is approximately 20 °C and the relative humidity is 55%); thus, all the samples could be considered to have followed a similar manufacturing and curing process. This method was chosen instead of immersing them in water in order to carry out a curing process similar to that of the prefabricated elements manufactured in factories. In general, precast manufacturing factories usually carry out the curing process in the open air, but inside an enclosed building or enclosure, similar to the one used in this research. This was carried out since the purpose of this mortar will be its possible use in these types of elements.

Figure 3. Curing of mortar samples (0.30 m × 0.30 m × 0.05 m).

Finally, the mortar samples were extracted from their moulds, taking care to avoid any damage by loosening and removing the screws holding the frame. A label with the corresponding code, which includes the sample number, was placed on each of the samples.

The time from the demoulding of the test samples to their use in the tests was 90 days. With this proposed curing method, it is possible to replicate the manufacturing conditions of serial prefabricated elements, as well as to make the curing conditions known so that they can be replicated by other authors.

2.3. Testing Method

This experiment analyses the thermal conductivity of different mortar samples with and without GOSs according to the procedure established by UNE-EN 12939:2001 ERRATUM:2009, "Thermal performance of building materials and products—Determination of thermal resistance by means of guarded hot plate and heat flow meter methods—Thick products of high and medium thermal resistance" [55].

Thermal conductivity (λ) is defined as the capacity of each material to transfer energy in the form of heat via conduction (direct contact, without exchange of matter) spontaneously and from the body with the highest temperature to the body with the lowest temperature. The unit used to measure thermal conductivity in the international system is W/m·K. Thermal conductivity is very high in metals (strong thermal conductors) and very low in insulating materials or polymers (thermal insulators).

2.3.1. GUNT WL 376

The machine used in this study to calculate thermal conductivity (λ) is model WL 376 (Figure 4) by the company GUNT Hamburg. In this case, the materials to be analysed are mortars doped with GOSs in different percentages.

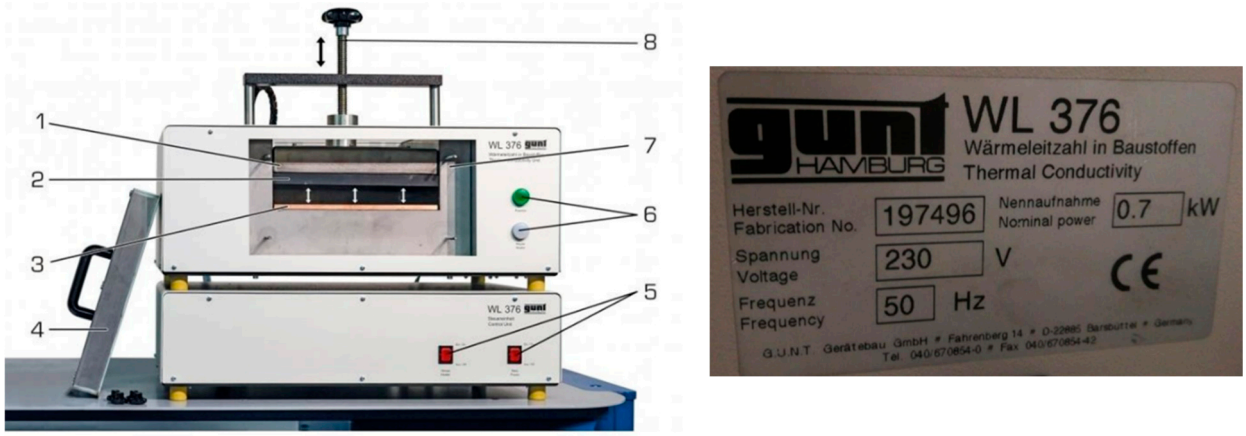

Figure 4. Thermal machine GUNT WL 376 and parts. 1. Hot plate insulation. 2. Hot plate. 3. Cold plate. 4. Cover for insulation casing. 5. Main switch and heat switch. 6. LED lights. 7. Insulation casing. 8. Pressure spindle.

The machine has a power of 500 W and can test 0.3 m × 0.3 m square samples on each side and up to a 0.05 m thickness, or a combination of different-sized samples as long as they do not exceed this thickness. The machine is capable of analysing all kinds of construction materials as long as they are not metallic.

After switching on the machine, the moving part of the machine raises to the stop, with the help of a spindle. Then, the sample is introduced without touching the cold plate or the hot plate to avoid damaging the sensors these plates have on their surface. Once the sample is in place, the hot plate is adjusted using the pressure spindle and rotated until it comes into contact with the cold plate, eliminating any air between the hot plate and the sample. Then, the cover of the insulation casing is closed to completely seal the system and, therefore, avoid any heat loss. To this end, fixed bolts must be inserted, and nuts are placed and tightened to prevent heat from escaping. And finally, the refrigerator is powered on, and the main water stopcock is opened to allow water to pass through and the cold plate to be cooled.

2.3.2. GUNT WL 376 Software Version 2.3

Next, the GUNT WL 376 software, version 2.3, included with the machine, is initiated, and the test data are entered on the main screen, called the 'system diagram':

- Hot plate temperature (30 °C, 40 °C, and 50 °C in three tests).
- Cold plate temperature (20 °C).
- Sample thickness (50 mm).

On this screen, the valve that allows the cooling water to pass through to the cold plate can also be opened. The 'Chart' screen indicates how the program should collect data (in this case, every 10 s). The temperature of the cold plate remains practically constant at 20 °C throughout; while the temperature of the hot plate varies. However, the cold plate's temperature does change slightly because as the hot plate's temperature varies, the refrigerator is not able to keep the cold plate at a constant temperature. Three tests are conducted on each of the samples while varying the working temperature: 20–30 °C, 20–40 °C, and 20–50 °C.

Pressing the start button creates a new data file that collects all the thermal conductivity (λ) values obtained until the test is terminated. At that point, the thermal conductivity is displayed on the 'System Diagram' screen, stabilises, and does not vary for at least 20 min to the second decimal place.

2.3.3. Obtaining the Parameter λ

The data obtained in the data file are exported to a spreadsheet, where all the values of λ are selected, which are constant, that is, at least the data collected during the last 20 min of testing. The thermal conductivity is tested to confirm whether it is consistent. If it is, the same cold plate temperature data interval is selected and plotted. If not, a data interval should be sought where λ is constant during the stipulated time. If this cannot be determined, the test must be repeated. Subsequently, the average temperature value is calculated, with the average temperature value of the cold plate (average of the selected data) and the temperature of the hot plate (data). These steps are carried out three times, once for each temperature range (20–30 °C, 20–40 °C, and 20–50 °C). Once the average value of the cold and hot temperatures and conductivity, λ, of each of the three temperature ranges are tested, the three points are plotted, the trend line is added, and the equation is obtained.

3. Thermal Results

This section begins by first explaining the results of the thermal conductivities obtained in the tests. This preliminary explanation of these results demonstrates the capacity of GOSs to reduce the thermal conductivity of the material in which they are embedded, in this case, mortar, and, consequently, to introduce their insulating capacity in a specific application such as prefabricated mortar elements applied to a new sustainable construction.

Table 5 shows the results obtained in the thermal test. Each value in the table is the arithmetic average of the results obtained for two samples of each batch (L1, L2, and L3) and their different doping percentages.

Table 5. λ conductivity values obtained for batches with different doping percentages.

	Thermal Conductivity, λ (W/m·k)		
Sample	**Batch 1 (L1)**	**Batch (L2)**	**Batch (L3)**
M-0	1.22	1.14	1.17
M-5	0.86	0.83	0.91
M-10	0.92	0.83	1.00
M-15	0.93	0.82	0.79
M-20	0.54	0.90	0.67
M-25	0.67	0.79	0.86
M-30	0.55	0.62	0.65

Based on the data obtained from the thermal samples, a third-degree polynomial regression curve is drawn to predict the value of thermal conductivity (λ) based on the percentage of GOSs included. In this sense, let us recall that a third-degree polynomial regression is the fit (based on the least squares) of a curve, with the expression described in (1)

$$y = a \cdot x^3 + b \cdot x^2 + c \cdot x + d \quad (1)$$

where a, b, c, and d are the parametric coefficients of the equation to calculate. To complete this equation, the average value of all the thermal conductivities obtained for the samples with the same percentage % of ground olive stones is used in order to obtain more uniform data. Figure 5 shows the graph obtained from the tests.

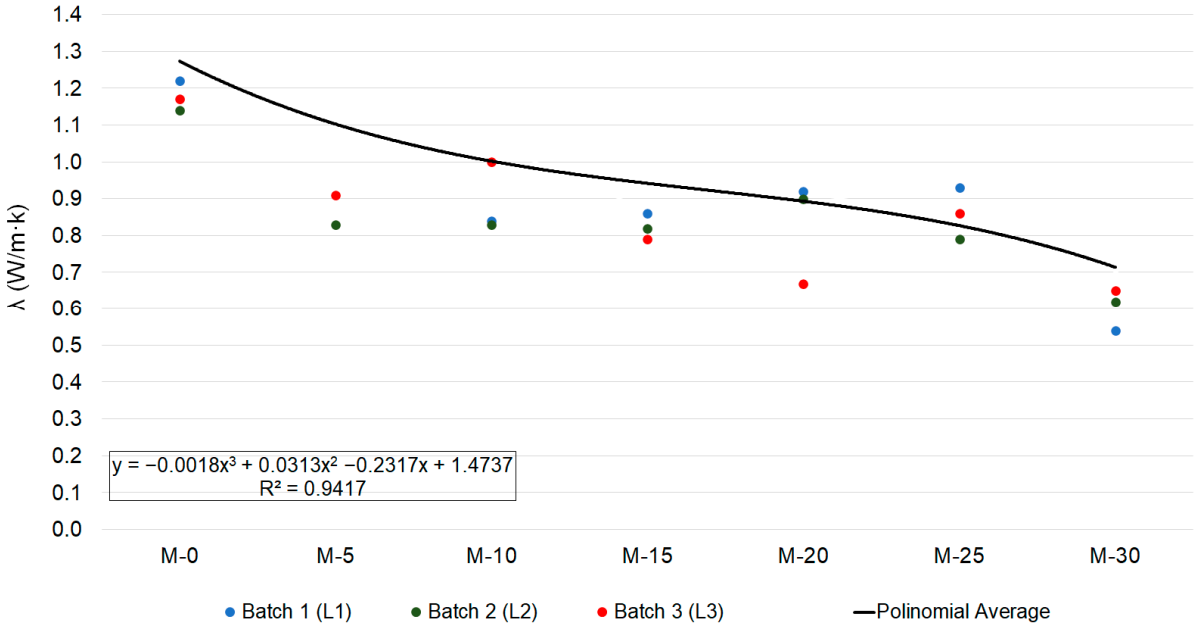

Figure 5. Third-degree polynomial regression curve of the results.

Equation (2) allows us to approximate the thermal conductivity (λ) of the mortars based on their percentage of olive stones:

$$\lambda\ (W/m \cdot K) = -0.0018 \cdot x^3 + 0.0313 \cdot x^2 - 0.2317 \cdot x + 1.4737 \quad (2)$$

where x is the percentage of olive stones added to the mixture, calculated as shown in (3).

$$x = (\%\ \text{Olive stone in mix}/5) + 1 \quad (3)$$

The relative predictive power of a polynomial model is denoted by the value of R2 (also known as the determination coefficient), which varies between 0 and 1 and is a statistical measure of how close the data are to the fitted regression. The closer the value is to 1, the more accurate the model in general, since the higher R2 is, the better the model fits the data. For the object of study herein, this value is 0.9417.

All the current energy efficiency directives approved by the European Union highlight environmental sustainability as a strategic pillar of energy policy. By adding a certain percentage of GOSs to mortar, the resulting thermal conductivity decreases proportionally, dropping by up to 43.94% compared to the non-doped mortar in the case of mortar with 30% olive stones.

4. Discussion

Comparing the results obtained with previous research shows a similar trend of results. For instance, the research by Barreca et al. obtained a thermal transmittance (U) value

of 36.10 W/m^2·K for a GOS percentage of 20%. In addition, the thickness (e) of the test specimen they used was 0.02 m [43].

$$U(W/m^2 \cdot K) = \lambda\ (W/m \cdot K)/e(m) \rightarrow \lambda = U \cdot e \quad (4)$$

Therefore, the value of the thermal conductivity (λ) can be obtained from (4) with a value of 0.722 W/m·K. In the results of the current investigation, the average value for a percentage of 20% was 0.703 W/m·K. This shows a decrease of 2.59% between the two studies. Figure 6 shows the comparative results obtained for thermal conductivity (λ) in comparison with those of the research by Barraca et al. [43].

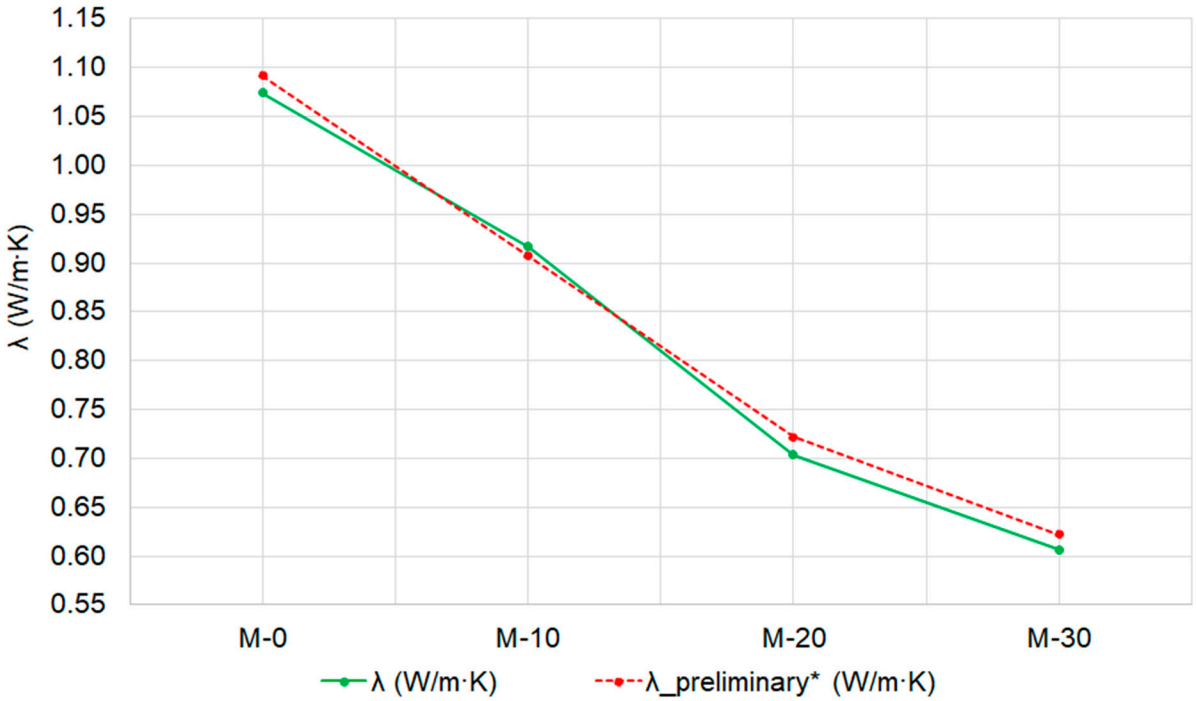

Figure 6. Comparison of thermal conductivities, λ (W/m·k). * [43].

As can be seen, the trend lines of the thermal conductivities (λ) are very similar for both studies. However, an improvement is observed in the current investigation for the thermal conductivities. This improvement is very small, ranging from 1.63% to 2.59%. On the other hand, for a doping of 10%, the research by Barraca et al. achieves an improvement in the thermal conductivity coefficient of 1.07% with respect to that obtained in this research [43]. This comparison is an attempt to justify the similar trend in the results obtained between the two studies, in addition to confirming the fact that GOSs can be considered a material that reduces the thermal conductivity coefficient.

Thus, incorporating GOSs into mortar not only reduces thermal conductivity but it is also capable of enhancing the thermal insulation of building enclosures. This type of mortar with a certain percentage of doping can be put to different uses in construction, such as the manufacturing of vaults, mortar bricks for façades or non-loaded partition walls, lightening pieces, or even thermal insulation with layers of mortar coating. However, this research will focus on its use in mortar bricks. Incorporating such elements would translate into a reduced energy demand for buildings, along with a subsequent decrease in CO_2 emissions and overall energy savings. Repurposing an abundant source of waste, such as olive stones, also renders such applications very interesting from an environmental and social sustainability standpoint.

5. Case Study: Energy Simulation of the Application of Mortar Bricks with GOSs

This energy simulation aims to determine the reduction in combined energy demand (heating and cooling) that occurs in a façade-type SATE. The results are compared with the traditional way of using GOS waste, that is, its combustion to obtain thermal energy.

Given the satisfactory results obtained for the coefficient of thermal conductivity (λ) and in order to assess the possible practical benefits of mortar doped with GOSs, an energy simulation study is conducted with a model of a new building that meets the current Technical Building Code [56]. The Technical Building Code stipulates energy demands according to the different climate zones in Spain. All the resulting models are calculated with the LIDER-CALENER Unified Tool version 2.0.2412.1173 [57]. This software is authorized by the Spanish Ministry for the Ecological Transition and Demographic Challenge to assign energy certifications to buildings and to inform the demand requirements and energy consumption levels included in the Technical Building Code.

To prepare the prototype, a residential block of flats is chosen, as outlined in model 6.2 of the document "Energy qualification of existing IDAE buildings" [58]. A model plan is used with a main façade of 21 m to the south and the rear to the north, and a 20 m perpendicular partition wall (east and west) in a quasi-square shape. Two small patios measuring 4 × 4 (16 m^2 each) open onto the two dividing façades. The 3D volumetric model is shown in Figure 7.

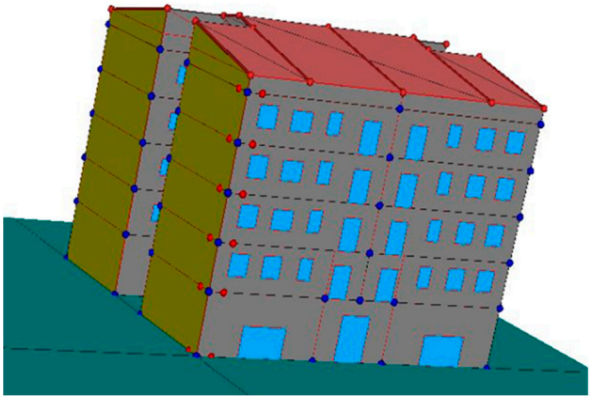

Figure 7. The 3D Building model.

The block of flats used in the simulation consists of

- A ground floor: 4 m-high mezzanine and ground floor with common access and two commercial premises.
- Four residential floors: 4 flats per floor measuring about 90.75 m^2 per flat (3 m of height between floors).
- A top floor with an inclined roof: storage rooms and lift machine room.

The thermal enclosure of the building consists of a set of enclosures (floors, roofs, façades, etc.) that separate the living spaces from the exterior (ground, air, and other buildings) and the interior partition walls that separate the habitable spaces from the non-habitable ones, which in turn are in contact with the outside. The enclosure of the modelled building includes the following types of enclosures shown in Table 6.

The objective is to calculate the reduction in combined heating and cooling energy demand (kWh/m^2 and year) from replacing two 11.5 cm-thick GERO brick sheets of conventional perforated mortar (according to the calculation software database) in the façade with another type of GERO brick of the same characteristics but with a percentage of GOSs.

The perforated GERO bricks have circular or diamond-shaped holes. The total volume of the perforations is between 25% and 50% of the total volume of the brick. Figure 8 shows an example of a perforated GERO brick.

Table 6. Total area of thermal enclosure of the building.

Element	Area (m^2)
Façades	988.52
Space	175.08
Partitions	569.60
Roofs	395.71
Floors in contact with Earth	388
Total	2516.91

Figure 8. Example of perforated GERO brick.

The following table specifies the thermal conductivity of the mortar brick (both solid and perforated) measuring 25 cm × 11.5 cm × 10 cm, according to the Catalogue of Construction Elements of the Technical Building Code in Spain [59] for mortar with a density of 2000 kg/m^3. The following values, as shown in Table 7, are used as a reference in this study.

Table 7. Values of for mortar, according to the CTE. Source: Construction Elements Catalogue [59].

Material	Dimensions (cm)	Mortar Density (kg/m^3)	λ (W/m·K)
Solid Brick	25 × 11.5 × 10	2000	1.714
Perforated GERO Brick	25 × 11.5 × 10	2000	1.091

The solid brick used for the calculation has a total volume of 2875 cm^3 of mortar. In the perforated GERO brick, the mortar volume decreases to 1603.3 cm^3, as it has a total of 18 holes of 3 cm in diameter. The percentage (%) mortar volume of the total brick is 55.77%. Therefore, the % volume of the holes is 44.23%. Likewise, the conductivity reduction coefficient due to air gaps between the solid brick and the perforated brick is 0.64.

The rest of the elements in the enclosure (the windows, doors, dividing walls, roofs, and floors in contact with the ground) are not modified during the simulation. They are, however, adapted to the requirements included in the Technical Building Code [56] according to Spain's five different climate zones. Figure 9 shows the existing climate zones in Spain.

The façade under study herein is a SATE façade, which is an exterior thermal insulation system consisting of a prefabricated insulating panel attached to a brick wall (in this case, expanded polystyrene, EPS) that is mechanically fixed with adhesive or anchors. The insulation is protected with an external coating consisting of a 3 cm layer of mortar that also incorporates a reinforcing mesh and is applied directly to the insulating panel without air gaps or a discontinuous layer. For the present study, the composition of the enclosure of the SATE façade (exterior thermal insulation system) for the building simulation is as follows:

- 1. A 3 cm-thick layer of mortar with λ = 1.254 W/m·K.
- 2. Extended polystyrene insulation with λ = 0.037 W/m·K of variable thickness depending on the climate region:

- Zone A (Almería): 4 cm
- Zone B (Sevilla): 5 cm
- Zone C (Barcelona): 8 cm
- Zone D (Logroño): 11 cm
- Zone E (Soria): 12 cm

- 3. A perforated GERO brick that is 11.5 cm thick with λ = 1.097 W/m·K.
- 4. A 2 cm-thick vertical air chamber without ventilation.
- 5. A perforated GERO brick that is 11.5 cm thick with λ = 1.097 W/m·K.
- 6. Plaster finish, 2 cm-thick.

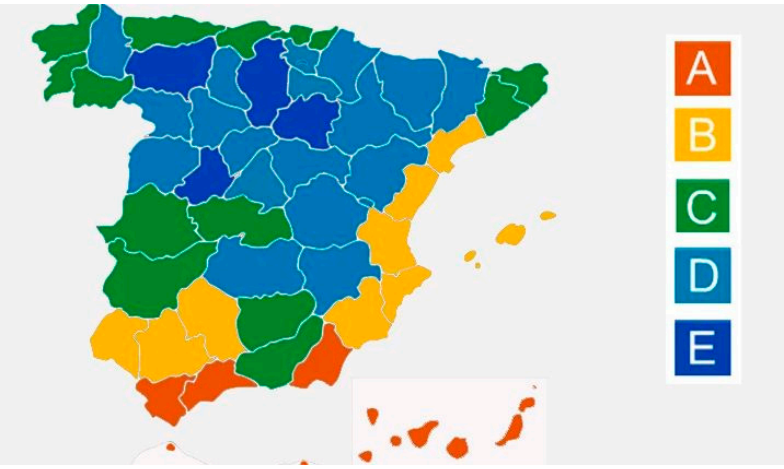

Figure 9. Climate zones according to the Spanish Technical Building Code.

Layers 3 and 5 are modified in the simulations with a GERO perforated brick from the program database with another of the same dimensions and characteristics but with the addition of 5%, 10%, 15%, 20%, 25%, and 30% GOSs and with the conductivity values obtained in the tests multiplied by the coefficient 0.64 (conductivity ratio between the perforated brick and the solid brick).

A key aspect that must be fulfilled is that the thermal transmittance (U) of the façade for the various cases of study must be lower than the maximum allowable thermal transmittance (U_{MAX}) established by the Technical Building Code according to its climatic zone. This U_{MAX} parameter is imposed in the DA DB-HE1 document [56]. These values are shown in Table 8, as along with the values of the thermal transmittances (U) for each case of study evaluated, including for the façade configuration, in which there is no doping of the mortar bricks. As can be seen, in no case is this limit value exceeded.

Table 8. Values of the total thermal transmittances (W/m^2·K) for each doping percentage and reference percentage as well as the maximum admissible transmittances, U_{MAX} (W/m^2·K), depending on the climatic zone.

Climate Zone	U_{MAX} (W/m^2·K)	U_{REF} (W/m^2·K)	$U_{5\%}$ (W/m^2·K) λ = 0.676	$U_{10\%}$ (W/m^2·K) λ = 0.603	$U_{15\%}$ (W/m^2·K) λ = 0.551	$U_{20\%}$ (W/m^2·K) λ = 0.510	$U_{25\%}$ (W/m^2·K) λ = 0.477	$U_{30\%}$ (W/m^2·K) λ = 0.449
A—Almería	0.500	0.410	0.389	0.383	0.378	0.373	0.369	0.365
B—Sevilla	0.380	0.369	0.352	0.347	0.343	0.339	0.335	0.332
C—Barcelona	0.290	0.284	0.274	0.271	0.268	0.266	0.264	0.262
D—Logroño	0.270	0.231	0.224	0.222	0.220	0.219	0.217	0.216
E—Soria	0.230	0.217	0.211	0.209	0.208	0.206	0.205	0.204
Total area of façade replaced: 988.52 m^2								

Therefore, multiple thermal simulations are carried out to calculate the reduction in the combined annual heating and cooling demand (kWh/m^2 and year), replacing the

conventional perforated GERO brick with another brick doped with GOSs in the 988.52 m^2 façade of the modelled building. The results obtained are shown in Table 9. As can be seen, the first column of Table 9 refers to the different climatic zones in Spain according to the Technical Building Code [56]. The second column corresponds to the sum of the heating and cooling demands for the reference case study building. In this case, the façade does not have any type of insulation. The remaining columns show, depending on the percentage of GOS doping in the GERO perforated bricks, the combined energy savings in heating and cooling. Therefore, to find out, for example, the total energy demand of the building for a climate zone type E in which the doping percentage is 20%, it is necessary to subtract from the reference energy demand of 54,391.8 kWh/year the energy savings that are produced with a doping percentage of 20%, which is equivalent to a value of 788.1 kWh/year. The result is 53,603.7 kWh/year, which is equivalent to a decrease of 1.45% in energy demand.

Table 9. Total annual energy savings (988.52 m^2 façade) thanks to the incorporation of olive stones, according to climate zones. * The reference demands (kWh/year) are the sum of the heating and cooling demands for the whole building and for the reference case where the mortar bricks are undoped.

	Combined Energy Savings for Heating and Cooling (kWh per Year)						
		Perforated Brick with % Doping					
Climate Zone	**Reference Demand ***	**5% λ = 0.676**	**10% λ = 0.603**	**15% λ = 0.551**	**20% λ = 0.510**	**25% λ = 0.477**	**30% λ = 0.449**
A—Almería	32,208.8	399.9	515.4	612.5	696.0	772.4	843.8
B—Sevilla	40,952.0	469.0	608.1	720.0	826.3	918.0	1006.4
C—Barcelona	33,536.9	431.5	553.1	659.4	761.3	855.5	934.7
D—Logroño	45,841.2	381.3	495.6	589.9	690.5	772.5	858.6
E—Soria	54,391.8	442.8	567.0	669.1	788.1	884.6	990.8
Total area of façade replaced: 988.52 m^2							

The best results in terms of the percentage reduction in the combined heating and cooling demand occur in the case of climate zone type C and in the specific case of 30% doping. In this case, the energy demand is reduced by 2.787%. On the other hand, the worst reduction percentage occurs in the case of a climate zone type E and in the case in which the bricks are doped with a minimum percentage of 5%. For this configuration, the percentage of reduction in the demand is 0.814%. Finally, it should be noted that the average value for the five climatic zones gives a percentage reduction in demand of 1.726%.

As can be seen, the energy savings of the combined thermal demand for heating and cooling (kWh and year) are greater for the higher percentages of doping, but the amount of GOSs that must be incorporated into the mortar is also greater. Table 10 shows, for the modelled façade, the average energy savings ratio (in five climate zones) as a function of the doping percentage. These energy savings include heating and cooling demands.

Table 10. Average energy savings per m^2 of façade thanks to the incorporation of ground olive stones.

Combined Energy Savings for Heating and Cooling (kWh per Year)						
Average energy savings per m^2 of façade	Perforated brick with % doping					
	5%	10%	15%	20%	25%	30%
	0.430	0.554	0.658	0.761	0.850	0.938

Once the energy savings in the building façade are known, they are compared with the traditional use of GOSs. GOSs are usually combusted in a biomass boiler. This comparison is carried out in order to know how long it would take to recover the energy in the building instead of burning it.

A lower calorific value is used for GOSs of 4489 kWh/kg, according to the document "Lower calorific values of primary energy sources" by the IDAE [60]. And a useful energy performance of 75% in combustion is considered, thereby quantifying losses in the boiler and in heat distribution. Taking into account the amount of GOSs added to each type of mortar, the following values are obtained for useful heat energy, as shown in Table 11.

Table 11. Equivalent useful energy from olive stone combustion * Façade surface area: 988.52 m^2; ** PCI olive stone (kWh/kg): 4489.

Mortar Type	Quantity of GOSs per m^2 Façade (kg/m^2) *	Total GOSs in Façade (kg)	Combustion Energy PCI Olive Stone (kWh) **	Useful Energy with Combustion Performance of 75% (kWh)
M-5	4.27	42,220.30	18,944.91	14,208.68
M-10	8.65	8546.30	38,364.33	28,773.24
M-15	12.73	12,579.81	56,470.76	42,353.07
M-20	17.01	16,817.55	75,494.00	56,620.50
M-25	21.25	21,008.18	94,305.73	70,729.30
M-30	26.69	26,383.85	118,437.10	88,827.83

And lastly, the combustion energy recovery time is considered in conjunction with the savings derived from the reduced combined heating and cooling demand generated by doping the mortar. The values obtained are displayed in Figure 10.

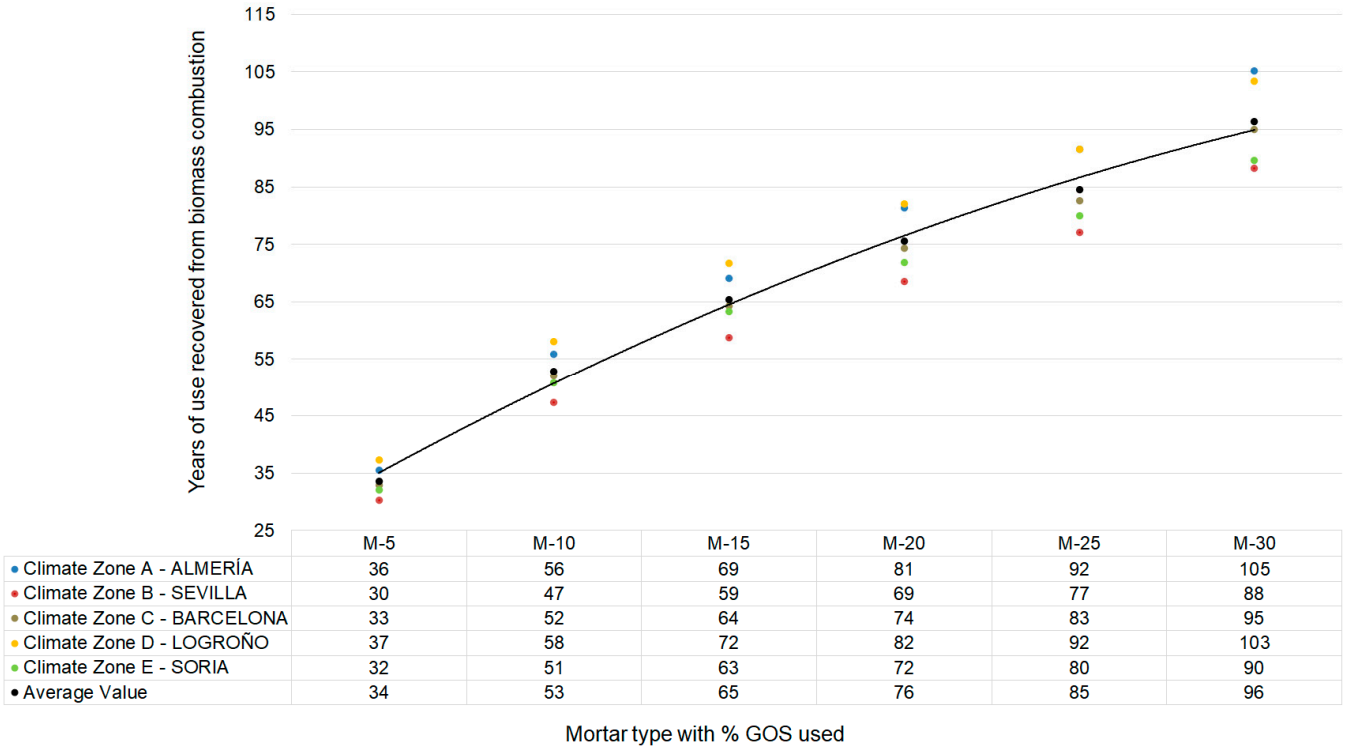

	M-5	M-10	M-15	M-20	M-25	M-30
Climate Zone A - ALMERÍA	36	56	69	81	92	105
Climate Zone B - SEVILLA	30	47	59	69	77	88
Climate Zone C - BARCELONA	33	52	64	74	83	95
Climate Zone D - LOGROÑO	37	58	72	82	92	103
Climate Zone E - SORIA	32	51	63	72	80	90
Average Value	34	53	65	76	85	96

Figure 10. Years of use recovered thanks to façade made with ground-olive-stone-doped mortar (26.5 cm thick) rather than combustion combined heating and cooling demand.

As can be observed, the best results are obtained with doping between 5% and 15%, where the average recovery period ranges from 30 to 70 years within the useful life of a building built in compliance with current regulatory requirements. It is concluded, therefore, that incorporating GOSs to manufacture a doped mortar and adding it to perforated bricks for façades makes it possible to recover, within the useful lifetime of a building, the useable energy that can be obtained by combusting olive stone in a biomass boiler.

Thus, this application offers benefits in terms of energy savings while also recycling an agricultural waste product: ground olive stones.

In view of the results shown in this research, future lines of research on the use of GOSs in mortar bricks for the manufacturing of sustainable façades will focus on analysing its economic, social, and environmental costs. In other words, they will evaluate the economic profitability of using this waste in prefabricated elements in a hypothetical industrial production, in addition to evaluating its social impact and assessing whether there is any social advantage, such as the generation of new jobs. And finally, future research should environmentally characterise, through the Life Cycle Analysis (LCA) tool, the possible environmental benefits of producing prefabricated mortar elements doped with GOSs.

6. Conclusions

The most significant conclusions obtained from this research are shown below.

The replacement of a volume percentage of fine aggregates by GOSs in mortars implies a decrease in the coefficient of thermal conductivity (λ) of the mortar. Specifically, for an additive doping of 5%, this reduction is 15.66%. This is equivalent to reducing a thermal conductivity value of 1.26 W/m·K to a final value of 1.05 W/m·K.

In addition, the research shows that the higher the doping percentage, the greater the influence it has on the reduction in the thermal conductivity coefficient (λ). This is particularly relevant in the case of a doping percentage of 30%, where the thermal conductivity coefficient (λ) decreases to a value of 0.607 W/m·K, which is 43.94% less than the reference value.

The anomalies and oscillations shown in the graphs are due to the moisture that the GOSs and fine aggregates absorb from the environment before manufacturing; hence, there is a need to carry out several test batches in order to obtain average values with minimal deviations.

Due to the rewarding results obtained in terms of the reduction in the thermal conductivity coefficient (λ), specific uses for this agricultural waste are proposed, such as the elaboration of mortar bricks for the manufacturing of more sustainable façades. In this way, a new way of using this agricultural waste is proposed in addition to the traditional way of using it as a source of biomass.

The results of the building energy simulation support the feasibility of incorporating GOSs in mortar bricks for the manufacturing of sustainable façades, where two façade leaves are composed of GOS-doped mortar bricks. For example, in the specific case where the bricks are doped with 5% GOS, there are savings in combined heating and cooling demands of 0.43 kWh per square metre of façade on an annual basis. And for a doping value of 30%, there is an energy saving of 0.938 kWh/m^2·year.

This reduction in the energy demands of heating and cooling for new buildings implies avoiding the consumption of traditional fossil fuels, such as natural gas, to meet these demands or reducing the consumption of electricity. This is associated with a reduction in CO_2 emissions and the sustainability of the sector.

Finally, the energy savings obtained by using GOSs in mortar bricks for sustainable façades were compared with the most common way of using this agricultural waste today, which is to obtain thermal energy in boilers. The results show a recovery range of 30 to 70 years (depending on the utilisation rate of GOSs).

The most viable outcome of this payback period is to dope the GERO perforated brick with 5% GOS, as it has a payback period between 30 and 37 years, which is approximately half of a building's lifetime (50~75 years).

This research has demonstrated the feasibility of using agricultural waste such as GOSs in the construction sector due to their improved thermal properties in their application to mortar bricks that reduce the energy demands (heating and cooling) of a new building. An alternative use for this agricultural waste is proposed, establishing future lines of research such as economic, social, and environmental analyses.

Author Contributions: Conceptualization, A.S.V.-N., M.M.-G., E.F.-G. and J.F.-C.; methodology, A.S.V.-N., E.F.-G. and J.F.-C.; software, A.S.V.-N., J.L.S.-O., M.M.-G., E.F.-G. and J.F.-C.; validation, M.M.-G., E.F.-G. and J.F.-C.; formal analysis, A.S.V.-N., M.M.-G., E.F.-G. and J.F.-C.; investigation, A.S.V.-N., J.L.S.-O., M.M.-G., E.F.-G. and J.F.-C.; resources, A.S.V.-N., J.L.S.-O., M.M.-G., E.F.-G. and J.F.-C.; data curation, A.S.V.-N. and J.L.S.-O.; writing—original draft preparation, A.S.V.-N. and J.L.S.-O.; writing—review and editing, A.S.V.-N. and J.L.S.-O.; visualization, M.M.-G., E.F.-G. and J.F.-C.; supervision, M.M.-G., E.F.-G. and J.F.-C.; project administration, E.F.-G. and J.F.-C.; funding acquisition, M.M.-G., E.F.-G. and J.F.-C. All authors have read and agreed to the published version of the manuscript.

Funding: This research was funded by University of La Rioja, grant number REGI2023/2021. Also the author Jorge Los Santos is a pre-doctoral researcher funded by the University of La Rioja and the Santander Bank.

Data Availability Statement: Data are contained within the article.

Acknowledgments: We are very grateful to the University of La Rioja, and the company Trujal 5 Valles for their support.

Conflicts of Interest: The authors declare no conflict of interest.

References

1. Andersen, M.S. An introductory note on the environmental economics of the circular economy. *Sustain. Sci.* **2007**, *2*, 133–140. [CrossRef]
2. Meyer, C. The greening of the concrete industry. *Cem. Concr. Compos.* **2009**, *31*, 601–605. [CrossRef]
3. Malhotra, V.M. Global Warming, and role of supplementary cementing materials and superplasticisers in reducing greenhouse gas emissions from the manufacturing of Portland cement. *Int. J. Struct. Eng.* **2010**, *1*, 116–130. [CrossRef]
4. Chen, L.; Huang, L.; Hua, J.; Chen, Z.; Wei, L.; Osman, A.I.; Fawzy, S.; Rooney, D.W.; Dong, L.; Yap, P.S. Green construction for low-carbon cities: A review. *Environ. Chem. Lett.* **2023**, *21*, 1627–1657. [CrossRef]
5. Georgiades, M.; Shah, I.H.; Steubing, B.; Cheeseman, C.; Myers, R.J. Prospective life cycle assessment of European cement production. *Resour. Conserv. Recycl.* **2023**, *194*, 106998. [CrossRef]
6. Fraile-Garcia, E.; Ferreiro-Cabello, J.; López-Ochoa, L.M.; López-González, L.M. Study of the technical feasibility of increasing the amount of recycled concrete was used in ready-mix concrete production. *Materials* **2017**, *10*, 817. [CrossRef] [PubMed]
7. Halahla, M.A.; Akthar, N.M.; Almasri, H.A. Utilization of Demolished Waste as Coarse Aggregate in Concrete. *Civ. Eng. J.* **2019**, *5*, 540–551. [CrossRef]
8. Akhtar, N.M.; Jameel, M.; Ibrahim, Z.; Bunnori, M.N. Incorporation of recycled aggregates and silica fume in concrete: An environmental savior-a systematic review. *J. Mater. Res. Technol.* **2022**, *20*, 4525–4544. [CrossRef]
9. Junaid, F.M.; Rehman, U.Z.; Kuruc, M.; Medved, I.; Bacinskas, D.; Curperk, J.; Cekon, M.; Ijaz, N.; Ansari, W.S. Lightweight concrete from a perspective of sustainable reuse of waste byproducts. *Constr. Build. Mater.* **2022**, *319*, 126061. [CrossRef]
10. European Commission. Waste Framework Directive (2008/98/EC)-European Environment Agency. Available online: https://www.eea.europa.eu/policy-documents/waste-framework-directive-2008-98-ec (accessed on 28 March 2023).
11. European Parliament. EUR-Lex-32002L0091-EN-EUR-Lex. Available online: https://eur-lex.europa.eu/legal-content/es/TXT/?uri=CELEX%253A32002L0091 (accessed on 28 March 2023).
12. Parracha, J.L.; Santos, A.R.; Lazera, R.; Colen, F.I.; Gomes, M.G.; Rodrigues, A.M. Performance of lightweight thermal insulating mortars applied on brick substrate specimens and prototype wall. *Constr. Build. Mater.* **2023**, *364*, 129954. [CrossRef]
13. Francesco, T.; Andrea, P.; Giusy, S.; Sabino, D.G.; Michele, N. Environmental Sustainable Cement Mortars Based on Polyethylene Terephtalate from Recycling Operations. *Materials* **2023**, *16*, 2111.
14. Ronnakrit, K.; Ampol, W.; Jindarat, E.; Piti, S.; Vanchai, S.; Prinya, C. Performance of Geopolymer Mortar Containing PVC Plastic Waste from Bottle Labels at Normal and Elevated Temperatures. *Buildings* **2023**, *13*, 1031.
15. De Melo, A.B.; Silva, E.P. Bloques de hormigón ligero con áridos reciclados de EVA: Una contribución a la eficiencia térmica de paredes exteriores de edificios. *Mater. De Construcción* **2013**, *63*, 479–495. [CrossRef]
16. Yesilata, B.; Isker, Y.; Turgut, P. Thermal insultation enhancement in concretes by adding waste PET and rubber pieces. *Constr. Build. Mater.* **2009**, *23*, 1878–1882. [CrossRef]
17. García, E.; Mauricio, P.; Schwarz, A.; César, A.; Urbano, B.; Medina, C. Environmental evaluation of applications of concrete with recycled material from tyre. In *Proceedings of the Institution of Civil Engineers-Engineering Sustainability*; Thomas Telford Ltd.: London, UK, 2022.
18. García, E.F.; Cabello, J.F.; Giro, M.M.; Navarro, S.V. Thermal behaviour of hollow blocks and bricks made of concrete doped with waste tyre rubber. *Constr. Build. Mater.* **2018**, *176*, 193–200. [CrossRef]
19. Dashti, P.; Ranjbar, S.; Ghafari, S.; Ramezani, A.; Nejad, F.M. RSM-based and environmental assessment of eco-friendly geopolymer mortars containing recycled waste tire constituents. *J. Clean. Prod.* **2023**, *428*, 139365. [CrossRef]

20. Letelier, V.; Bustamante, M.; Olave, B.; Martínez, C.; Ortega, M. Properties of mortars containing crumb rubber and glass powder. *Dev. Built Environ.* **2023**, *14*, 100131. [CrossRef]
21. Eskander, B.S.; Saleh, M.H.; Tawfik, E.M.; Bayoumi, A.T. Towards potential applications of cement-polymer composites based on recycled polystyrene foam wastes on construction fields: Impact of exposure to water ecologies. *Case Stud. Constr. Mater.* **2021**, *15*, e00664. [CrossRef]
22. Mebarkia, R.; Bouzeroura, M.; Chelouah, N. Study of the effect of cement kiln dust on the mechanical, thermal and durability properties of compressed earth blocks. *Constr. Build. Mater.* **2022**, *349*, 128707. [CrossRef]
23. Gencel, O.; Kazmi, S.M.S.; Munir, M.J.; Sutcu, M.; Erdogmus, E.; Yaras, A. Feasibility of using clay-free bricks manufactured from water treatment sludge, glass, and marble wastes: An exploratory study. *Constr. Build. Mater.* **2021**, *298*, 123843. [CrossRef]
24. Belhadj, B.; Bederina, M.; Montrelay, N.; Houessou, J.; Quéneudec, M. Effect of substitution of wood shavings by barley straws on the physico-mechanical properties of lightweight sand concrete. *Constr. Build. Mater.* **2014**, *66*, 247–258. [CrossRef]
25. Brás, A.; Antunes, A.; Préneron, L.A.; Ralegaonkar, R.; Shaw, A.; Riley, M.; Faria, P. Optimisation of bio-based building materials using image analysis method. *Constr. Build. Mater.* **2019**, *223*, 544–553. [CrossRef]
26. Moghadam, S.A.; Roshan, G.M.A.; Omidinasab, F. Utilization of agricultural wastes as fiber, binder and aggregates of geopolymer mortars: Application of Taguchi method for strength and durability optimization. *J. Build. Eng.* **2023**, *75*, 106906. [CrossRef]
27. Pilien, V.P.; Promentilla, B.A.M.; Leaño, L.J.; Oreta, C.W.A.; Ongpeng, C.M.J. Confinement of Concrete Using Banana Geotextile-Reinforced Geopolymer Mortar. *Sustainability* **2023**, *15*, 6037. [CrossRef]
28. Kamsuwan, T. The Mechanical Properties for Using Banana's Peel Ash as Aggregate in Geopolymer Mortar. *Lect. Notes Civ. Eng.* **2023**, *279*, 70–76.
29. Akinyemi, A.B.; Dai, C. Development of banana fibers and wood bottom ash modified cement mortars. *Constr. Build. Mater.* **2020**, *241*, 118041. [CrossRef]
30. Sathiparan, N.; Anburuvel, A.; Selvam, V.V. Utilization of agro-waste groundnut shell and its derivatives in sustainable construction and building materials—A review. *J. Build. Eng.* **2023**, *66*, 105866. [CrossRef]
31. Wang, Q.; Li, S.J.; Poon, S.C. Productive of sorptive granules from incinerated sewage sludge ash and upcycling in cement mortars. *Sep. Purif. Technol.* **2023**, *309*, 123046. [CrossRef]
32. Lakreb, N.; Sen, U.; Beddiar, A.; Zitoune, R.; Nobre, C.; Gomes, M.G.; Pereira, H. Properties of eco-fiendly mortars produced by partial cement replacement with waste cork particles: A feasibility study. *Biomass Convers. Biorefinery* **2023**, *13*, 11997–12007. [CrossRef]
33. Boubakour, S.; Kherraf, L.; Hebhoub, H.; Messaoudi, K.; Boukhatem, G. Characterization of lightweight mortars with cork and olive stone waste for old building rehabilitation. *Ann. De Chim. Sci. Des Mater.* **2023**, *47*, 179–185. [CrossRef]
34. Malchiodi, B.; Marchetti, R.; Barbieri, L.; Pozzi, P. Recovery of cork manufacturing waste within mortar and polyurethane: Feasibility of Use and Physical, Mechanical, Thermal Insulating Properties of the Final Green Composite Construction Materials. *Appl. Sci.* **2022**, *12*, 3844. [CrossRef]
35. Olaiya, C.B.; Lawan, M.M.; Olonade, A.K. Utilization of sawdust composites in construction-a review. *Appl. Sci.* **2023**, *5*, 140. [CrossRef]
36. Bishetti, P.; Varadharajan, S.; Shukla, B.K.; Bharti, G. Study on suitability of sawdust as an alternate for fine aggregate in concrete. *Lect. Notes Civ. Eng.* **2023**, *281*, 209–217.
37. Barbuta, M.; Mihai, P.; Precul, A.M.N.; Bejan, L.; Taranu, N.; Banu, M.O. Concrete hollow blocks with waste materials replacing the natural aggregates. *Rev. Romana Mater.* **2022**, *52*, 83–89.
38. Gudia, S.E.L.; Go, A.W.; Giduquio, M.B.; Juanir, R.G.; Jamora, J.B.; Gunarto, C.; Tabañag, I.D.F. Surgarcane bagasse ash as a partial replacement for cement in paste and mortar formulation-A case in the Philippines. *J. Build. Eng.* **2023**, *76*, 107221. [CrossRef]
39. Madhanagopal, A.; Arunkumar, S.; Jagatheesan, K.; Adinarayanan, A. Investigation on mechanical and thermal properties of clay brick additions with sugarcane bagasse ash and nanoparticles. *Biomass Convers Biorefinery* 2023. [CrossRef]
40. Hussien, N.T.; Oan, F.A. The use of sugarcane wastes in concrete. *J. Eng. Appl. Sci.* **2022**, *69*, 31. [CrossRef]
41. Prayuda, H.; Monika, F.; Passa, A.S.; Lubis, A.R.; Wibowo, E.D. Engineering properties of mortar with untreated agricultural waste ashes as cement replacement materials. *Innov. Infrastruct. Solut.* **2023**, *8*, 227. [CrossRef]
42. Khan, M.A.; Khan, A.S.; Khan, B.; Shahzada, K.; Althoey, F.; Deifalla, F.A. Investigating the feasibility of producing sustainable and compatible binder using marble waste, fly ash, and rice husk ash: A comprehensive research for material characteristics and production. *Results Eng.* **2023**, *20*, 101435. [CrossRef]
43. Barreca, F.; Fichera, C.R. Use of olive stone as an additive in cement lime mortar to improve thermal insultation. *Energy Build.* **2013**, *62*, 507–513. [CrossRef]
44. Ince, C.; Tayancli, S.; Derogar, S. Recycling waste wood in cement mortars towards the regeneration of sustainable environment. *Constr. Build. Mater.* **2021**, *299*, 123891. [CrossRef]
45. Conde, M.M.J.; Rubio-de-Hita, P.; Gálvez, P.F. Composite mortars produced with Wood waste from demolition: Assessment of new compounds with enhanced thermal properties. *J. Mater. Civ. Eng.* **2018**, *30*, 04017273. [CrossRef]
46. Pokorny, J.; Sevcik, R.; Sal, J.; Fiala, L.; Zarybnicka, L.; Podolka, L. Bio-based aggregate in the production of advanced thermal-insulating concrete with improved acoustic performance. *Constr. Build. Mater.* **2022**, *358*, 129436. [CrossRef]
47. Anuario. Available online: https://www.mapa.gob.es/es/estadistica/temas/publicaciones/anuario-de-estadistica/2021/default.aspx (accessed on 29 June 2023).

48. Abdelhamid, A.A.; Badr, H.M.; Mohamed, A.R.; Saleh, M.H. Using Agricultural Mixed Waste as a Sustainable Technique for Removing Stable Isotopes and Radioisotopes from the Aquatic Environment. *Sustainability* **2023**, *15*, 1600. [CrossRef]
49. Cabello, J.F.; Garcia, E.F.; Espinoza, A.P.; Martínez de Pison, F.J. Strength Performance of Different Mortar Doped Using Olive Stone as Lightweight Aggregate. *Buildings* **2022**, *12*, 1668. [CrossRef]
50. UNE-EN 933-1:2012. Available online: https://www.en.une.org/encuentra-tu-norma/busca-tu-norma/norma?c=N0049638 (accessed on 5 May 2023).
51. UNE 7 133. Available online: https://books.google.es/books/about/UNE_7_133.html?id=P6VyswEACAAJ&hl=e (accessed on 26 June 2023).
52. UNE-EN 1744-1:2010. Available online: https://www.une.org/encuentra-tu-norma/busca-tu-norma/norma?c=N0051093 (accessed on 26 June 2023).
53. UNE-EN 1097-6:2014. Available online: https://www.une.org/encuentra-tu-norma/busca-tu-norma/norma?c=N0052839 (accessed on 26 June 2023).
54. UNE-EN 12350-2:2002. Available online: https://www.une.org/encuentra-tu-norma/busca-tu-norma/norma?c=N0063378 (accessed on 6 November 2023).
55. UNE-EN 12939:2001. Available online: https://www.une.org/encuentra-tu-norma/busca-tu-norma/norma?c=N0044070 (accessed on 29 March 2023).
56. Ministerio de Transporte, Movilidad y Agenda Urbana. Código técnico de la Edificación (CTE). Available online: https://www.codigotecnico.org/ (accessed on 29 March 2023).
57. Herramienta Unificada LIDER-CALENER. Available online: https://www.codigotecnico.org/Programas/HerramientaUnificadaLIDERCALENER (accessed on 28 March 2023).
58. Insitituto para la Diversifiación y Ahorro de la Energía. Escala de Calificación Energética. Edificios Existentes. Available online: https://www.idae.es/uploads/documentos/documentos_11261_EscalaCalifEnerg_EdifExistentes_2011_accesible_c762988d.pdf (accessed on 28 March 2023).
59. Ministerio de Transporte, Movilidad y Agenda Urbana. Digital Catalogue of Construction Elements. Available online: https://www.codigotecnico.org/Programas/CatalogoElementosConstructivos.html (accessed on 8 February 2023).
60. Spanish Institute for Energy Diversification and Savings. Lowe Calorific Values of Primary Energy Sources. Available online: https://www.google.com/search?q=idae+poderes+calorificos&client=firefox-b-d&ei=VdojZIXxOvOikdUP-p2EqAY&oq=IDAE+poderes&gs_lcp=Cgxnd3Mtd2l6LXNlcnAQARgAMgUIABCA (accessed on 29 March 2023).